Characterization of the Polysilicon Resistor in Silicon Strip Sensors for ATLAS Inner Tracker as a Function of Temperature, Pre- And Post-Irradiation

V. Latoňová[a,b,*], P.P. Allport[c], E. Bach[d], J. Bernabeu[e], A. Chisholm[c], V. Cindro[f], V. Fadeyev[g], P. Federičová[a], J. Fernandez-Tejero[h,i], W. George[c], L. Gonella[c], K. Hara[j], S. Hirose[j], T. Ishii[j], T. Knight[k], I. Kopsalis[c], J. Kroll[a], J. Kvasnička[a], C. Lacasta[e], J. Lomas[c], I. Mandić[f], M. Mikeštíková[a], R.S. Orr[k], E. Rossi[k], C. Solaz[e], U. Soldevila[e], M. Ullan[d], Y. Unno[l]

[a] *Academy of Sciences of the Czech Republic, Institute of Physics, Na Slovance 2, 18221 Prague 8, Czech Republic*
[b] *Faculty of Mathematics and Physics, Charles University, V Holesovickach 2, Prague, CZ18000, Czech Republic*
[c] *School of Physics and Astronomy, University of Birmingham, Birmingham B152TT, United Kingdom*
[d] *Centro Nacional de Microelectronica (IMB-CNM, CSIC), Campus UAB-Bellaterra, 08193 Barcelona, Spain*
[e] *Instituto de Física Corpuscular, IFIC/CSIC-UV, C/Catedrático José Beltrán 2, E-46980 Paterna, Valencia, Spain*
[f] *Experimental Particle Physics Department, Jožef Stefan Institute, Jamova 39, SI-1000 Ljubljana, Slovenia*
[g] *Santa Cruz Institute for Particle Physics (SCIPP), University of California, Santa Cruz, CA 95064, USA*
[h] *Department of Physics, Simon Fraser University, 8888 University Drive, Burnaby, B.C. V5A 1S6, Canada*
[i] *TRIUMF, 4004 Wesbrook Mall, Vancouver, B.C. V6T 2A3, Canada*
[j] *Institute of Pure and Applied Sciences, University of Tsukuba, 1-1-1 Tennodai, Tsukuba, Ibaraki 305-8571, Japan*
[k] *Department of Physics, University of Toronto, 60 Saint George St., Toronto, Ontario M5S1A7, Canada*
[l] *Institute of Particle and Nuclear Study, High Energy Accelerator Research Organization (KEK), 1-1 Oho, Tsukuba, Ibaraki 305-0801, Japan*

Abstract

The high luminosity upgrade of the Large Hadron Collider, foreseen for 2029, requires the replacement of the ATLAS Inner Detector with a new all-silicon Inner Tracker (ITk). The expected ultimate total integrated luminosity of 4000 fb^{-1} means that the strip part of the ITk detector will be exposed to the total particle fluences and ionizing doses reaching the values of $1.6 \cdot 10^{15}$ 1 MeV $\mathrm{n_{eq}/cm^2}$ and 0.66 MGy, respectively, including a safety factor of 1.5. Radiation hard $\mathrm{n^+}$-in-p micro-strip sensors were developed by the ATLAS ITk strip collaboration and are produced by Hamamatsu Photonics K.K. The active area of each ITk strip sensor is delimited by the n-implant bias ring, which is connected to each individual $\mathrm{n^+}$ implant strip by a polysilicon bias resistor. The total resistance of the polysilicon bias resistor should be within a specified range to keep all the strips at the same potential, prevent the signal discharge through the grounded bias ring and avoid the readout noise increase. While the polysilicon is a ubiquitous semiconductor material, the fluence and temperature dependence of its resistance is not easily predictable, especially for the tracking detector with the operational temperature significantly below the values typical for commercial microelectronics.

Dependence of the resistance of polysilicon bias resistor on the temperature, as well as on the total delivered fluence and ionizing dose, was studied on the specially-designed test structures called ATLAS Testchips, both before and after their irradiation by protons, neutrons, and gammas to the maximal expected fluence and ionizing dose. The resistance has an atypical negative temperature dependence. It is different from silicon, which shows that the grain boundary has a significant contribution to the resistance. We discuss the contributions by parameterizing the activation energy of the polysilicon resistance as a function of the temperature for unirradiated and irradiated ATLAS Testchips.

Keywords: HL-LHC, ATLAS ITk, Silicon micro-strip sensor, Polysilicon bias resistor, Testchip
2010 MSC: 82-06, 82D37

ATL-ITK-PROC-2022-004
29 June 2022

1. Introduction

By 2026 the current ATLAS Inner Detector (ID)[1] will reach the end of its lifetime as it will not be able to cope with the harsh radiation environment, pile-up, occupancies and data transfer connected with the installation of the high luminosity upgrade of the Large Hadron Collider (HL-LHC). Thus, the ID will be replaced by a new all-silicon Inner Tracker (ITk) designed to withstand the high radiation damage associated with the anticipated ultimate total integrated luminosity of 4000 fb^{-1} accumulated during the expected operational time of more than 10 years. During the lifetime of HL-LHC the strip part of the ITk will be exposed to the total particle fluences of $1.6 \cdot 10^{15}$ 1 MeV $\mathrm{n_{eq}/cm^2}$ together with the total ionizing doses of 0.66 MGy including the safety factor of 1.5. For this pur-

*Corresponding author
Email address: vera.latonova@cern.ch (V. Latoňová)

pose, radiation hard n^+-in-p micro-strip sensors were developed by the ATLAS ITk strip collaboration and are manufactured by Hamamatsu Photonics K.K. [2]. The active area of the micro-strip sensor contains high number of n^+ implant strips, each of which is connected via the polysilicon bias resistor to the n-implant bias ring, running along the sensor's active area and keeping all strips on the same potential. Concerning the value of the bias resistance, it is desirable that the value is high enough to minimize the parallel thermal noise contribution and that the strip to strip differences are sufficiently low in order to avoid voltage deviations among strips and non-uniform field distribution.

Polysilicon, as the name implies, is a polycrystalline form of silicon comprising of many small randomly oriented crystallites (grains). It is assumed that the energy band structure known for single-crystalline silicon, including the activation energy $E_a^{\text{silicon}} = 1.21\,\text{eV}$ [3], can be applied inside the individual crystallites. However, the electrical properties of polysilicon are believed to be mostly determined by effects at the grain boundary, such as trapping and immobilization of charge carriers [4].

2. Irradiation And Measurement Procedure

The study was carried out on 17 Testchips [5] identified by the batch and the wafer numbers, e.g. VPX32483-W00001. The samples were irradiated by protons, neutrons and gammas at different irradiation sites. The proton irradiation was performed at the University of Birmingham [6], UK by 27 MeV and at CYRIC [7], Japan by 70 MeV protons, the irradiation by neutrons took place at Ljubljana JSI TRIGA reactor [8] and the gamma irradiation was achieved by ^{60}Co source at UJP Praha [9].

The Testchips were measured in temperature range between $-50\,°\text{C}$ and $+25\,°\text{C}$ either wire-bonded on PCBs in an environmental chamber or placed on thermal chuck of a probe station and contacted by needles.

The bias resistance for each temperature was obtained indirectly from I-V scans as $R_{\text{bias}} = \left(\frac{\text{d}I}{\text{d}V}\right)^{-1}$.

3. Results I.: Temperature Dependence And Activation Energy

Temperature Dependence of R_{bias}. From the measured data it can be shown that the dependence of R_{bias} on temperature is exponential and can be thus described by the Eq. (1):

$$R_{\text{bias}}(T) = R_0 \cdot \exp\left(\frac{E_a}{2kT}\right), \qquad (1)$$

where E_a is the activation energy of polysilicon and k is the Boltzmann constant.

The exponential dependence can be proven by displaying the measured data in Arrhenius-like plot (Figure 1), in which we plot the logarithm of the ratio of R_{bias} and R_0 against reciprocal of the scaled temperature.

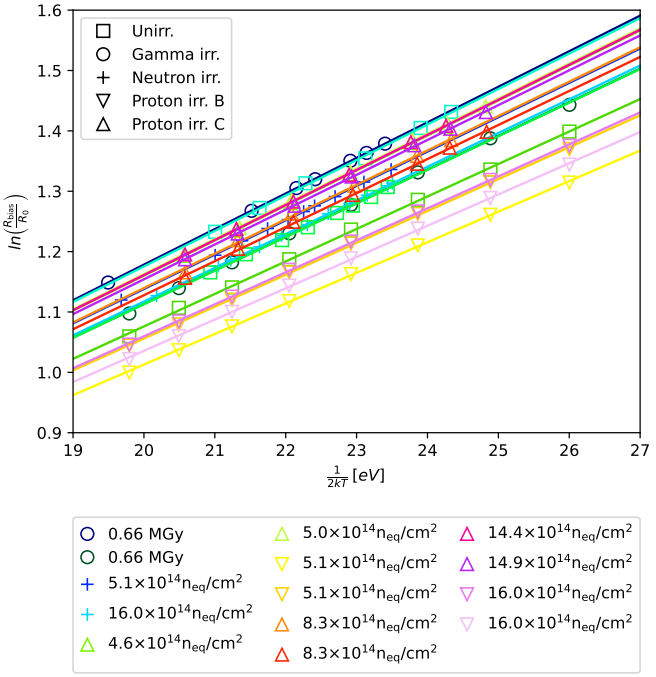

Figure 1: Arrhenius-like plot of R_{bias} values vs temperature. The values for Testchips irradiated by different particles to various irradiation levels are denoted by markers and the corresponding linear fits are plotted as solid lines.

Activation Energy of Polysilicon. The fits of Arrhenius-like plots in Figure 1 are linear and nearly parallel to each other, which implies that the polysilicon bias resistance is characterized by a single activation energy. The value of the activation energy for each sample was obtained by fitting the measured R_{bias} data using the Eq. (1). The results for different irradiation types are shown in Tables 1 to 4, from which it is obvious that the activation energy is independent of irradiation type. Slight deviations in individual values are caused by different set-ups used at testing sites and are in accordance with previously published results in [10].

The activation energy of polysilicon was determined as the average value of the obtained activation energies $E_a^{\text{polysilicon}} = (55.8 \pm 0.1) \cdot 10^{-3}\,\text{eV}$.

Table 1: Activation energy (E_a) measured for for unirradiated Testchips.

Testchip (Batch-Wafer)	$E_a[\cdot 10^{-3}\,\text{eV}]$
VPX32483-W00001	58.7 ± 1.1
VPX33426-W00082	55.6 ± 0.9
VPX34148-W00201	53.8 ± 0.6

Table 2: Activation energy (E_a) measured for gamma irradiated Testchips.

Testchip (Batch-Wafer)	TID [MGy]	$E_a[\cdot 10^{-3}\,\text{eV}]$
VPX32418-W00144	0.66	58.9 ± 0.2
VPX33426-W00073	0.66	55.7 ± 0.6

Table 3: Activation energy (E_a) measured for neutron irradiated Testchips.

Testchip (Batch-Wafer)	Fluence [$\cdot 10^{14}$ n_{eq}/cm^2]	$E_a[\cdot 10^{-3}$ eV]
VPX32421-W00371	5.1	56.9 ± 0.3
VPX32426-W00367	16.0	55.9 ± 0.2

Table 4: Activation energy (E_a) measured for proton irradiated Testchips. The symbols ^{B} and ^{C} denote Testchips irradiated at Birmingham and at CYRIC, respectively.

Testchip (Batch-Wafer)	Fluence [$\cdot 10^{14}$ n_{eq}/cm^2]	$E_a[\cdot 10^{-3}$ eV]
VPX32423-W80366^C	4.6	58.0 ± 0.2
VPX32587-W00064^C	5.0	58.1 ± 0.6
VPA37915-W00314^B	5.1	50.6 ± 0.3
VPA37915-W00306^B	5.1	52.8 ± 0.4
VPA37915-W00295^C	8.3	57.0 ± 1.4
VPX37425-W00755^C	8.3	56.4 ± 0.6
VPX32425-W00317^C	14.4	58.1 ± 0.5
VPX32471-W00051^C	14.9	57.7 ± 0.3
VPA37915-W00333^B	16.0	53.0 ± 0.4
VPA37915-W00340^B	16.0	51.8 ± 0.4

4. Prediction of Temperature Development of R_{bias} for Various Irradiations

In the previous section it has been shown that the temperature dependence of R_{bias} can be described by Eq. (1) and that the activation energy as a material constant has the same value for all samples. Now, for one chosen sample we set $R_{\mathrm{bias}} = R_m$ at a temperature T_m. Then, from Eq. (1) we get for R_0 relation (2):

$$R_0 = \frac{R_m}{\exp\left(\frac{E_a}{2kT_m}\right)} \tag{2}$$

By inserting Eq. (2) into Eq. (1) we obtain for all other samples:

$$\begin{aligned} R(T;T_m,R_m) &= \frac{R_m}{\exp\left(\frac{E_a}{2kT_m}\right)} \exp\left(\frac{E_a}{2kT}\right) \\ &= R_m(T_m)\cdot \exp\left(\frac{E_a}{2k}\left(\frac{1}{T}-\frac{1}{T_m}\right)\right) \end{aligned} \tag{3}$$

Measured R_{bias} values of each Testchip were compared with a curve obtained from Eq. (3), in which we used for R_m the bias resistance value at temperature $-20\,^{\circ}\mathrm{C}$ and for the activation energy we used the value $E_a = = 53.8 \cdot 10^{-3}$ eV obtained from the fit for one of the unirradiated Testchips. From Figure 2 it is apparent that within the examined temperature range the R_{bias} values obtained from Eq. (2) match very well with the measured results.

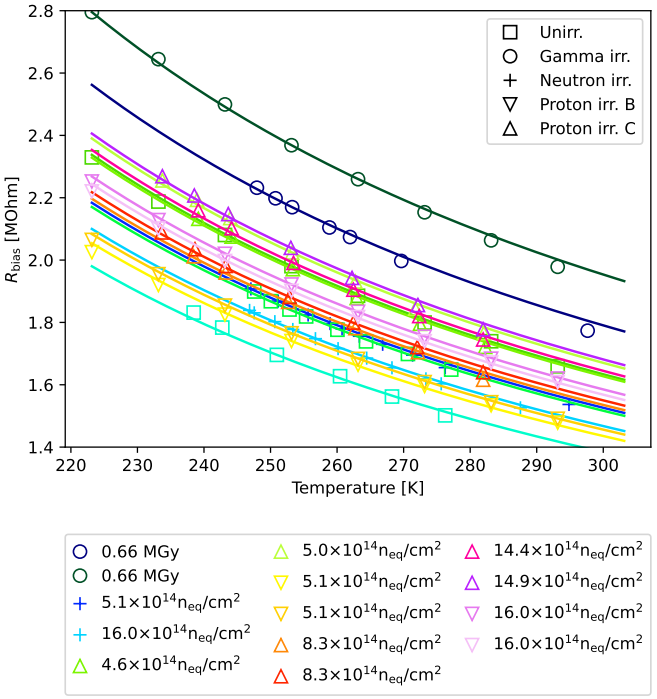

Figure 2: Calculated temperature dependence of R_{bias} (solid lines) compared with the measured R_{bias} values (markers).

5. Results II.: Dependence of R_{bias} on Total Ionizing Dose (TID) And Fluence

R_{bias} vs fluence. The fluence dependence of the R_{bias} values measured for samples irradiated by protons and neutrons is shown in Figure 3. Neglecting the slight span in individual measured values, which is present already for unirradiated samples and is in accordance with [10], we do not see any correlation between the measured R_{bias} values and fluence for protons or neutrons.

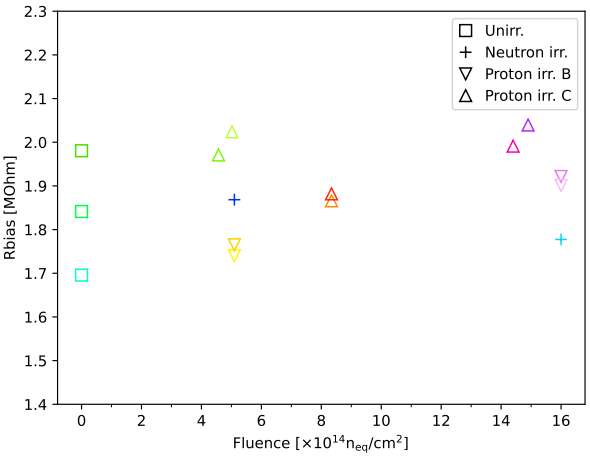

Figure 3: Dependence of R_{bias} on fluence.

In Figure 4 the ratio of two R_{bias} values of the same sample measured at temperatures $-20\,^{\circ}\mathrm{C}$ and $-10\,^{\circ}\mathrm{C}$ vs

the total delivered fluence is plotted.

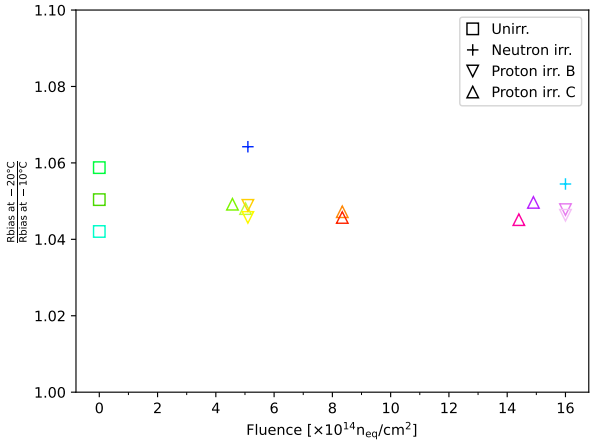

Figure 4: Ratio of two R_{bias} values of the same sample measured at temperatures −20 °C and −10 °C vs fluence.

R_{bias} vs TID. In order to study the dependence of R_{bias} on TID it was necessary to convert the proton and neutron fluence into TID. The proton irradiation was converted to TID using the formula (4):

$$\text{TID} = \frac{\Phi}{\kappa}\left(\frac{\mathrm{d}E}{\mathrm{d}x}\right)_{E_p}, \tag{4}$$

where Φ is the proton fluence in 1 MeV neutron equivalent, $\left(\frac{\mathrm{d}E}{\mathrm{d}x}\right)_{E_p}$ is the stopping power of protons with energy E_p in silicon taken from Ref. [11] and κ is the hardness factor (κ is 1.552 and 2.2 for CYRIC and Birmingham, respectively). The TID in neutron irradiated Testchips caused by secondary particles has been assessed to be 100 krad per $1 \cdot 10^{14}\,\text{n}_{\text{eq}}/\text{cm}^2$. The dependence of R_{bias} on TID is presented in Figure 5, where we do not observe any significant change of R_{bias} with TID for any of the three irradiation types (protons, neutrons or gammas). The source of the slightly higher R_{bias} values in case of gamma irradiated Testchips compared to the samples irradiated by protons and neutrons is under investigation.

Figure 6 shows the ratio of two R_{bias} values of the same sample at temperatures −20 °C and −10 °C, from which it is apparent that the activation energy does not change with irradiation.

6. Conclusions

Dependence of the resistance of polysilicon bias resistor on temperature and irradiation was studied on several ATLAS ITk Testchips that were specially designed to have the same properties as the large-format micro-strip sensors, which will be installed in the ATLAS ITk detector in HL-LHC.

It has been shown that the value of polysilicon bias resistance decreases as $\exp\left(\frac{E_a}{2kT}\right)$ with temperature. By fitting

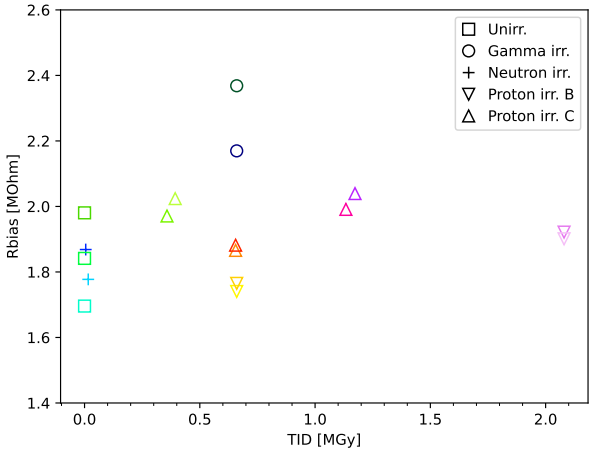

Figure 5: Dependence of R_{bias} on TID.

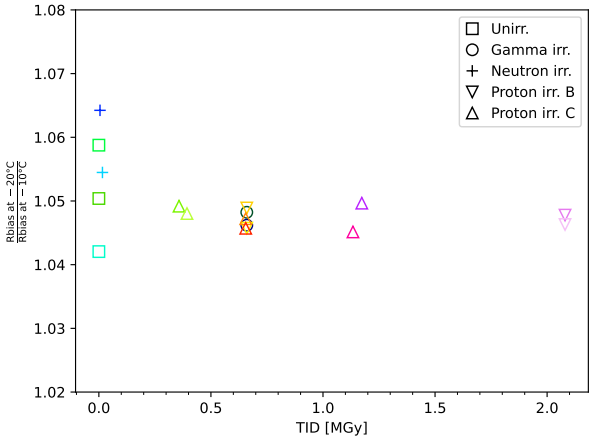

Figure 6: Ratio of two R_{bias} values of the same sample at temperatures −20 °C and −10 °C vs TID.

the values of R_{bias} measured at different temperatures by the Formula (1) we determined the activation energy of polysilicon as $E_a^{\text{polysilicon}} = (55.8 \pm 0.1) \cdot 10^{-3}$ eV, which differs from the activation energy of single-crystalline silicon (1.21 eV) and thus implies that the electrical properties of polysilicon are governed by charge carriers trapping and other effects at the grain boundary.

Further, by using Eq. (3), it was possible to determine the temperature evolution of R_{bias} for any studied sample based on one value of bias resistance R_m measured at a temperature T_m . This result was verified in Figure 2.

It has been also shown that for a given temperature, the value of R_{bias} does not change with fluence or TID and thus also the activation energy does not depend on the type and level of irradiation.

7. Acknowledgments

This work was supported by the Ministry of Education, Youth and Sports of the Czech Republic via the projects LTT17018 Inter-Excellence and LM2018104 CERN-CZ,

Charles University grant GAUK 942119, the Slovenian Research Agency (research core funding No. P1_0135), the Canada Foundation for Innovation and the Natural Sciences and Engineering Research Council of Canada, the US Department of Energy, grant DE-SC0010107, JSPS Grant-in-Aid for Research Activity Start-up 20K22346 and the Spanish R&D grant PID2019-110189RB-C22, funded by MCIN/ AEI/10.13039/501100011033. The authors would like to thank the crew at the TRIGA reactor in Ljubljana for help with the irradiation of the detectors.

References

[1] The ATLAS Collaboration, et al., The ATLAS experiment at the CERN large hadron collider, Journal of Instrumentation 3 (08) (2008) S08003–S08003. doi:10.1088/1748-0221/3/08/s08003.

[2] Y. Unno, et al., ATLAS17LS – A large-format prototype silicon strip sensor for long-strip barrel section of ATLAS ITk strip detector, Nucl. Instrum. Meth. A 989 (2021) 164928. doi:10.1016/j.nima.2020.164928.

[3] A. Chilingarov, Temperature dependence of the current generated in Si bulk, Journal of Instrumentation 8 (10) (2013) P10003–P10003. doi:10.1088/1748-0221/8/10/p10003.

[4] J. Y. W. Seto, The electrical properties of polycrystalline silicon films, Journal of Applied Physics 46 (1975) 5247–5254. doi:10.1088/1748-0221/8/10/p10003.

[5] M. Ullán, et al., Quality assurance methodology for the atlas inner tracker strip sensor production, Nuclear Instruments and Methods in Physics Research Section A: Accelerators, Spectrometers, Detectors and Associated Equipment 981 (2020) 164521. doi:10.1016/j.nima.2020.164521.

[6] P. Allport, et al., Recent results and experience with the birmingham MC40 irradiation facility, Journal of Instrumentation 12 (03) (2017) C03075–C03075. doi:10.1088/1748-0221/12/03/c03075.

[7] K. Nakamura, et al., Irradiation and testbeam of KEK/HPK planar p-type pixel modules for HL-LHC, Journal of Instrumentation 10 (06) (2015) C06008–C06008. doi:10.1088/1748-0221/10/06/c06008.

[8] Snoj, L., Ambrozic, K., et al., Radiation hardness studies and detector characterisation at the jsi triga reactor, EPJ Web Conf. 225 (2020) 04031. doi:10.1051/epjconf/202022504031.

[9] UJP PRAHA a.s., https://ujp.cz/en/, (Accessed on 05/13/2022).

[10] E. Bach, et al., Results from atlas-itk strip sensors quality assurance testchip, 12th International Conference on Position Sensitive Detectors (PSD12). Birmingham, UK, September 2021.

[11] Stopping power and range tables for protons, https://physics.nist.gov/cgi-bin/Star/ap_table.pl, (Accessed on 05/13/2022).